

Published in final edited form as:

ACS Appl Mater Interfaces. 2013 June 12; 5(11): 5208–5213. doi:10.1021/am401042u.

Photoconjugation of molecularly imprinted polymer with magnetic nanoparticles

Changgang Xu^{1,†}, Khan Mohammad Ahsan Uddin^{1,†}, Xiantao Shen¹, Surangi Jayawardena², Mingdi Yan², and Lei Ye^{1,*}

¹Division of Pure and Applied Biochemistry, Lund University, Box 124, 22100 Lund, Sweden

²Department of Chemistry, University of Massachusetts Lowell, 1 University Avenue, Lowell, MA 01854, USA

Abstract

Because of their synthetic accessibility, molecularly imprinted polymer (MIP) nanoparticles are ideal building blocks for preparing multifunctional composites. In this work we developed a general photo-coupling chemistry to enable simple conjugation of MIP nanoparticles with inorganic magnetic nanoparticles. We first synthesized MIP nanoparticles using propranolol as a model template and perfluorophenylazide-modified silica-coated magnetic nanoparticles. Using a simple photoactivation followed by facile purification with a magnet, we obtained magnetic composite particles that showed selective uptake of propranolol. We characterized the nanoparticles and composite materials using FT-IR, TEM, fluorescence spectroscopy and radioligand binding analysis. Through the high molecular selectivity of the magnetic composite, we demonstrated the non-destructive feature and the high efficiency of the photocoupling chemistry. The versatile photoconjugation method developed in this work should also be very useful for combining organic MIPs with other inorganic nanoparticles to enable new chemical sensors and high efficiency photo-catalysts.

Keywords

Molecular imprinting; photoconjugation; magnetic nanoparticles; molecular recognition; propranolol; perfluorophenylazide

1. Introduction

Molecular imprinting is a well-known technique to generate highly selective synthetic polymer receptors for target molecules. During the imprinting process, a monomer-template complex is formed through covalent or non-covalent interactions between the functional monomer and the template molecule in a pre-polymerization solution.^{1,2} After polymerization, the template is removed from the polymer matrix to create imprinted cavities with a size, shape and three-dimensional structure complementary to the template. Molecularly imprinted polymers (MIPs) display more advantages than antibodies and natural receptors, such as high chemical stability, high mechanical stability, ease of preparation and low cost. Recently, MIP nanoparticles have attracted increasing interest since they have more advanced properties than the conventional bulk MIPs, i.e. high surface area, fast binding kinetics, colloidal stability, synthetic accessibility and easy handling for

*Corresponding author: lei.ye@tbiokem.lth.se; Fax: +46 46 2224611; Tel: +46 46 2229560.

†These authors contributed equally to this work.

use in assays.³⁻⁵ Multifunctional composite materials prepared from different functional elements have attracted great interest because of their many practical applications. Combining MIPs with inorganic nanoparticles can lead to new chemical sensors,⁶⁻⁸ high efficiency photo-catalysts,^{9,10} and magnetic adsorbents useful for fast molecular separation.¹¹⁻¹³ Because of the advanced properties of MIP nanoparticles, they are ideal building blocks for preparation of multifunctional composites.

Recently, multifunctional MIP composites have been synthesized by our group using alkynyl-or azide-modified MIP core-shell nanoparticles as building blocks. The special core-shell structure allowed the MIP nanoparticles to be conjugated using the simple Huisgen 1,3-dipolar cycloaddition reaction (click chemistry). Although the conjugation strategy based on the click reaction was straightforward, it needed extra processes to introduce a “clickable” shell on the surface of MIP nanoparticles,^{14,15} which can be tedious and may affect the surface property of the MIP nanoparticles and bring in unexpected non-specific binding effect. The purpose of this work is to develop a new and simple conjugation chemistry that allows un-modified MIP nanoparticles to be easily linked to other functional materials. A photocoupling chemistry based on perfluorophenyl azide (PFPA) was selected because of its simplicity and general applicability of immobilizing organic materials.¹⁶⁻²⁸ Upon light activation, PFPA is converted to a highly reactive nitrene intermediate that can covalently link to organic materials through C-H, N-H insertion or C=C addition reactions.²⁴ This photo conjugation technique has been widely used in surface engineering and development of functional materials.²⁴ In this work, we investigate the suitability of the PFPA-based photoconjugation method for the preparation of MIP-based composite materials. As a model system, we study how ordinary MIP nanoparticles can be conjugated with magnetic nanoparticles to afford new affinity adsorbents through simple photochemical reactions.

2. Experimental section

2.1. Materials

Methacrylic acid (MAA, 98.5%), trimethylolpropane trimethacrylate (TRIM, technical grade), tetraethyl orthosilicate (TEOS, 99.99%), diethoxy(3-glycidyloxypropyl)methylsilane (DEGPMS), methyl pentafluorobenzoate, sodium azide, atenolol, poly(allylamine) solution (PAA, average MW ~17,000, 20 wt.% in H₂O) and *N*-hydroxysuccinimide (NHS) were purchased from Sigma Aldrich. Acetic acid (glacial, 100%), acetonitrile (99.7%) and azobisisobutyronitrile (AIBN, 98%) used for polymer synthesis were purchased from Merck (Darmstadt, Germany). AIBN was re-crystallized from methanol before use. (R,S)-Propranolol hydrochloride (99%) and (S)-propranolol hydrochloride (99%), supplied by Fluka (Dorset, UK), were converted into the free base form before use. (S)-[4-³H]-Propranolol (specific activity 555 GBq mmol⁻¹, 66.7 μM solution in ethanol) was purchased from NEN Life Science Products Inc. (Boston, MA). Scintillation liquid, Ecoscint A was from National Diagnostics (Atlanta, GA). All solvents were analytical grade and were used as received. PFPA-NHS was synthesized following a previously reported procedure.²⁹

2.2. Preparation of Propranolol-imprinted nanoparticles

Propranolol-imprinted nanoparticles were synthesized using precipitation polymerization following a procedure described by Yoshimatsu et al.³⁰ Briefly, the template molecule, (R,S)-propranolol (137 mg, 0.53 mmol) was dissolved in 40 mL of acetonitrile in a 150 mm × 25 mm borosilicate glass tube equipped with a screw cap. MAA (113 mg, 1.31 mmol), TRIM (648 mg, 2.02 mmol) and AIBN (28 mg) were then added. The solution was purged with a gentle flow of nitrogen for 5 min and then sealed. Polymerization was carried out by fixing the borosilicate glass tube horizontally in a Stovall HO-10 Hybridization Oven

(Greensboro, NC, USA), and rotated at a speed of 20 rpm, at 60°C for 24 h. After polymerization, polymer particles were collected by centrifugation at 13000 rpm ($16060 \times g$) for 20 min. The template was removed by washing with methanol containing 10% acetic acid (v/v) until no template could be detected from the washing solvent using UV spectrometric measurement. The polymer particles were finally washed with acetone and dried in a vacuum chamber. For comparison, non-imprinted polymer (NIP) nanoparticles were synthesized under the same condition but in the absence of the template.

2.3. Preparation of poly(allylamine)-coated magnetic nanoparticles ($\text{Fe}_3\text{O}_4@SiO_2@PAA$)

Epoxy-modified magnetic Fe_3O_4 nanoparticles ($\text{Fe}_3\text{O}_4@SiO_2@epoxy$) were synthesized using the same method as described previously by us.¹⁴ Briefly, FeCl_3 (7.30 g) and $\text{FeSO}_4 \cdot 7\text{H}_2\text{O}$ (8.35 g) were dissolved in 100 mL of water and heated to 80 °C. Ammonium hydroxide (25%, 30 mL) was then added. To improve the stability of the particle dispersion, a small amount of oleic acid (2 mL) was also added, resulting in the formation of oleic acid-coated magnetic nanoparticles. The reaction was allowed to last for 3 h under constant stirring before the Fe_3O_4 nanoparticles formed were collected using a magnet. The Fe_3O_4 nanoparticles were washed thoroughly with 95% ethanol for 3 times, distilled water 2 times, and then dried under vacuum overnight.

The Fe_3O_4 nanoparticles (1 g) were dispersed in a mixture of 80 mL ethanol (95%) and 20 mL of distilled water in a 250 mL flask. TEOS (2 mL) and ammonium hydroxide (2.5 mL) were then added at room temperature under vigorous mechanic stirring. The reaction proceeded for 24 h, and the $\text{Fe}_3\text{O}_4@SiO_2$ nanoparticles formed were then collected using a permanent magnet, washed with methanol and water, and then dried under vacuum overnight.

To introduce epoxy groups, the $\text{Fe}_3\text{O}_4@SiO_2$ nanoparticles (0.75 g) were dispersed in 10 mL toluene, followed by addition of 2 mL of DEGPMS. The mixture was heated to 50 °C and kept for 12 h under stirring. The epoxy-modified particles were then collected, washed with methanol and water, and dried under vacuum for 24 h. To obtain PAA-coated magnetic nanoparticles ($\text{Fe}_3\text{O}_4@SiO_2@PAA$), the epoxy-modified $\text{Fe}_3\text{O}_4@SiO_2$ nanoparticles (100 mg) were dispersed in a mixture of 3 mL of pyridine, 2.5 mL of distilled water and 0.5 mL of 20% polyallylamine. The reaction was then carried out at 50°C in the Stovall HO-10 Hybridization Oven for 5 h. After this reaction, the PAA-coated magnetic nanoparticles ($\text{Fe}_3\text{O}_4@SiO_2@PAA$) were collected and washed with water (5×10 mL), and finally dried in vacuum for 24 h.

2.4. Detection of amine groups of $\text{Fe}_3\text{O}_4@SiO_2@PAA$ particles

The amine groups on the magnetic $\text{Fe}_3\text{O}_4@SiO_2@PAA$ particles were detected using a method previously described by Uddin et al.³¹ Briefly, a stock solution of naphthalene-2,3-dicarboxaldehyde (NDA) (4 mM) was prepared in methanol. The stock solution was diluted with 0.1 M phosphate buffer (pH 8) to give 0.02 mM of NDA solution. A suspension of $\text{Fe}_3\text{O}_4@SiO_2@PAA$ in water (25 μl at 2 mg/ml) was mixed with 1 mL of the NDA solution and 1 mL of 0.02 mM KCN dissolved in 0.1 M phosphate buffer. The mixture was stirred for a few minutes at room temperature. After the NDA treatment, fluorescence emission of the mixture was measured with a QuantaMaster C-60/2000 spectrofluorometer (Photon Technology International, Lawrenceville, NJ, USA). The excitation wavelength was fixed at 418 nm for all the measurements. As a control, the $\text{Fe}_3\text{O}_4@SiO_2$ particles were also treated with the NDA reagent and the obtained mixture was subjected to the same fluorescence measurement.

2.5. Preparation of PFPA-coated magnetic nanoparticles ($\text{Fe}_3\text{O}_4@\text{SiO}_2@\text{PAA}@\text{PFPA}$)

$\text{Fe}_3\text{O}_4@\text{SiO}_2@\text{PAA}$ nanoparticles (50 mg) were dispersed in a 5 mL mixture of pyridine and water (v/v: 1:1), and 50 mg PFPA-NHS was then added to the mixture. The reaction was carried out at room temperature for 24 h in a glass tube protected from light. The magnetic nanoparticles were then collected and washed with water 3 times (3×5 mL), and dried under vacuum overnight.

2.6. Preparation of magnetic composites by photoconjugation

$\text{Fe}_3\text{O}_4@\text{SiO}_2@\text{PAA}@\text{PFPA}$ particles (20 mg) and MIP nanoparticles (20 mg) were suspended in 1 mL of acetone and homogenized by sonication. The suspension was then deposited in a Petri dish ($\varphi = 3$ cm). After the solvent was evaporated, the dried particles were photo-activated using a 450 W medium pressure mercury lamp for 10 min through a 280 nm optical filter (the distance between the UV lamp and the particles was 6 cm). The particles were then collected using a permanent magnet and washed repeatedly with acetone (2×1 mL) and water (3×1 mL), and dried under vacuum. As a control, a binary particle mixture composed of $\text{Fe}_3\text{O}_4@\text{SiO}_2@\text{PAA}@\text{PFPA}$ and the MIP nanoparticles was prepared with the photoconjugation step omitted, and the sample was subjected to the same washing steps, where a permanent magnet was used to collect the magnetic particles.

2.7. Analysis of organic content in the magnetic composites

Magnetic composites (30 mg) were mixed with 1 mL of hydrofluoric acid and stirred on a rocking table for 12 h. The remaining solid particles were then washed with acetonitrile (3×2 mL) and dried. The mass of the organic nanoparticles obtained were measured, and used to calculate the content of organic polymer in the composites.

2.8. FT-IR analysis

The presence of azide groups in the core-shell nanoparticles was confirmed by FT-IR analysis. Attenuated total reflection (ATR) infrared spectra were recorded on a Perkin-Elmer FT-IR instrument (Perkin-Elmer Instruments, Waltham, MA, USA). All spectra were collected in the $4000\text{--}375$ cm^{-1} region with a resolution of 4 cm^{-1} , with 32 scans, and at 25 $^\circ\text{C}$.

2.9. Radioligand binding analysis

In a series of polypropylene microcentrifuge tubes, magnetic composite particles (2 mg) were suspended in 1 mL of a mixture of 25 mM citrate buffer (pH 6.0): acetonitrile (50:50, v/v). After addition of (*S*)-[4- ^3H]-propranolol (246 fmol), the mixture was incubated at room temperature for 16 h. A rocking table was used to provide gentle mixing. After the incubation, the magnetic particles were precipitated using a permanent magnet for 5 min. Supernatant (500 μL) was withdrawn and mixed with 10 mL of scintillation liquid (Ecoscint A). The radioactivity of the samples was measured with a Tri-Carb 2810 TR liquid scintillation analyzer (PerkinElmer). The amount of radioligand bound to the polymer particles was calculated by subtracting the free radioligand from the total radioligand added. The data are mean values of measurements on three independent samples. Displacement experiments were carried out under the same condition, except that the amount of magnetic composite particles was fixed at 2.56 mg, and additional competing compounds ((*S*)-propranolol and atenolol) were added in the binding solvent.

3. Results and discussion

Propranolol-imprinted nanoparticles were synthesized by precipitation polymerization and showed high binding specificity, as has been reported in our previous publications.^{14,15,30}

These organic MIP nanoparticles were used as a model to demonstrate that the PFPA activated photoreaction can afford effective nanoparticle conjugation. Considering practical applications and the ease of material characterization, we decided to conjugate MIP nanoparticles with PFPA-modified magnetic nanoparticles, because successfully conjugated composite particles can be easily separated using a simple permanent magnet. The synthetic strategy of preparing the composite magnetic particles is shown in Scheme 1.

3.1. Preparation of PFPA-modified magnetic nanoparticles

To introduce the photoactive PFPA groups, magnetic Fe_3O_4 nanoparticles were first coated with a silica shell, followed by reacting with DEGPMS to introduce epoxy groups. The obtained magnetic nanoparticles were then reacted with poly(allylamine) through a ring-opening reaction to introduce a high density of amino groups on surface,²³ which reacted in a subsequent step with PFPA-NHS to furnish the surface bound PFPA groups (Scheme 1a). To confirm the presence of the surface bound amino groups on the $\text{Fe}_3\text{O}_4@SiO_2@PAA$ particles, the particles were treated with naphthalene 2,3-dicarboxaldehyde (NDA). As expected, the NDA reaction turned the amino-modified $\text{Fe}_3\text{O}_4@SiO_2@PAA$ into strongly fluorescent particles, whereas the two control samples (the NDA solution and the $\text{Fe}_3\text{O}_4@SiO_2$ particles treated with the NDA reagent) gave almost no background fluorescence (Fig. 1).

As shown in Fig. 2, the PFPA-modified magnetic nanoparticles ($\text{Fe}_3\text{O}_4@SiO_2@PAA@PFPA$) had a weak IR absorption band at 2115 cm^{-1} (curve 1, Fig. 2), which was also found in PFPA-NHS and could be assigned to the aromatic azide group. Although this IR band was weak due to the small quantity of the surface-bound PFPA, it was clearly visible in contrast to the IR spectrum of $\text{Fe}_3\text{O}_4@SiO_2@PAA$ (curve 2, Fig. 2). For both $\text{Fe}_3\text{O}_4@SiO_2@PAA$ and $\text{Fe}_3\text{O}_4@SiO_2@PAA@PFPA$, the characteristic IR bands for silica at 3279 cm^{-1} (H-bonded OH stretching), 1063 cm^{-1} (asymmetric vibration of Si-O), 950 cm^{-1} (asymmetric vibration of Si-OH) and 796 cm^{-1} (symmetric vibration of Si-O) were observed. Therefore, the IR analysis result indicates that PFPA has been successfully immobilized on the surface of the magnetic nanoparticles. In addition, the characteristic amide bands at 1490 cm^{-1} and 1660 cm^{-1} in the IR spectrum of $\text{Fe}_3\text{O}_4@SiO_2@PAA@PFPA$ (curve 1, Fig. 2) also support the successful immobilization of PFPA on the magnetic nanoparticles.

3.2. Preparation of composite MIP particles through photo-coupling reaction

The magnetic MIP composite particles were synthesized through conjugation of MIP nanoparticles with $\text{Fe}_3\text{O}_4@SiO_2@PAA@PFPA$ by photoactivated conjugation reaction (Scheme 1b). Considering the different sizes and densities of the two types of particles, the mass ratio between the MIP nanoparticles and the PFPA-modified magnetic nanoparticles was chosen as 1:1. To avoid possible side reactions between the organic solvent and the surface bound PFPA, the solvent was removed before the particle mixtures were subjected to photoactivation. This photoconjugation reaction was very efficient and could be finished in less than 10 min. The photoconjugated composite particles collected by a permanent magnet showed a strong IR absorption band at 1727 cm^{-1} (curve 2, Fig. 3), which was attributed to the carbonyl groups of the MIP nanoparticles (curve 4, Fig. 3). Besides, the IR band corresponding to the C=C double bond (at 2965 cm^{-1}) in the original MIP nanoparticles (curve 4, Fig. 3) decreased significantly after the photoconjugation (curve 2, Fig. 3), most likely due to the addition reaction between the C=C group and the photo generated nitrene intermediate. The above results suggest that the two types of nanoparticles were successfully conjugated. In a control experiment, a mixture of the two types of nanoparticles (without photoconjugation) was subjected to the same washing steps and collected using the same permanent magnet. In this case, most of the MIP nanoparticles

were lost, as indicated by the very weak IR absorption band at 1727 cm^{-1} (curve 3, Fig. 3). The two characteristic bands for the MIP (at 2965 cm^{-1} and 1727 cm^{-1}) were not observed in the IR spectrum of $\text{Fe}_3\text{O}_4@\text{SiO}_2@\text{PAA}@\text{PFPA}$ (curve 1, Fig. 3).

Fig. 4 shows TEM images of the MIP nanoparticles, the magnetic nanoparticles, and the composite particles obtained after the photoconjugation reaction. TEM analysis revealed that the size of the magnetic nanoparticles was $65 \pm 6\text{ nm}$, and the size of the MIP nanoparticles was $100 \pm 4\text{ nm}$. As seen in Fig. 4c, the photoconjugated composite particles contained both the smaller magnetic and the larger MIP nanoparticles that were covalently linked to each other. By inspecting additional TEM images, we could conclude that the size of the photoconjugated composite particles were in the range of $150 - 500\text{ nm}$. Based on the TEM image in Fig. 4c and the fact that the particles collected using permanent magnet displayed characteristic IR band of the MIP, we can conclude that the photoconjugation between the two types of nanoparticle building blocks was successful.

The magnetic MIP composite could be easily separated by applying an external magnetic field. As shown in Fig. 5, when a permanent magnet was applied, the composite particles could be quickly collected. This fast magnetic separation of all the solid particles also indicates that all the organic polymers were conjugated to the magnetic particles through the photocoupling reaction.

3.3. Molecular recognition of magnetic MIP composite

Because the conjugation reactions are confined on the interface between two nanoparticles, we expected that the majority of molecular recognition sites in the original MIP nanoparticles should remain intact during the photocoupling reaction. In this way, the MIP nanoparticles should still maintain high selectivity for the original template. To verify this hypothesis, we used radioligand binding analysis to compare the uptake of propranolol by the MIP and the NIP composite particles. Before the radioligand binding experiment, the content of the organic nanoparticles in the composite materials was determined by gravimetric measurement, where the inorganic silica and Fe_3O_4 were removed from the composite by treatment in HF. The results indicate that the imprinted composite and the non-imprinted composite contained 19.5% and 18% organic polymer, respectively. As the MIP and the NIP composites have very similar organic content, it is possible to judge if the specific binding observed in the original MIP nanoparticles can survive the photoconjugation reaction by comparing directly the different uptake of propranolol by the two types of composite particles. The two composites were incubated with [^3H]-(*S*)-propranolol in acetonitrile: citrate buffer (50: 50) to test their binding for the radioligand. As shown in Fig. 6a, while the MIP composite (containing $\sim 0.39\text{ mg}$ MIP nanoparticles) could bind 22% of the radioligand, the uptake by the NIP composite (containing 0.36 mg NIP nanoparticles) was only 2.4%. The fact that the MIP composite maintained high specific binding for the original template indicates that very few of the imprinted sites have been affected by the photoconjugation. The very low non-specific binding displayed by the NIP composite also suggests that the PFPA-modified magnetic nanoparticles did not bring in additional non-specific adsorption. The molecular selectivity of the MIP composite was further verified by comparing the capability of (*S*)-propranolol and atenolol to displace the labeled (*S*)-propranolol from the composite particles. As shown in Fig. 6b, while (*S*)-propranolol could effectively displace the radioligand from the MIP composite, atenolol showed almost no effect. This clear difference observed between propranolol and its structural analog (atenolol) confirms that the MIP composites maintained very high molecular selectivity.

4. Conclusions

In this work, we have developed a novel approach to prepare molecularly imprinted composite materials using simple and highly efficient photo-conjugation chemistry. With this new method, molecularly imprinted organic polymer was easily conjugated to perfluorophenylazide (PFPA)-modified magnetic nanoparticles by photo-activation. As the nanoparticle conjugation only involved coupling reactions on the particle surface, the specific binding sites in the imprinted organic polymer remained intact. As a result, the obtained magnetic MIP composites maintained high molecular selectivity and could be easily separated by applying an external magnetic field. Based on the results obtained in this model study, we believe that the photocoupling chemistry based on PFPA can provide a convenient means for preparing multifunctional composite materials from modular MIPs and other types of inorganic nanoparticles (e.g. gold nanoparticles, quantum dots and TiO₂ nanoparticles), which may allow new MIP-based chemical sensors and catalysts to be realized.

Acknowledgments

This work was supported by the Swedish Research Council FORMAS, the Danish Council for Strategic Research (project FENAMI, DSF-10-93456), and the US National Institute of Health (2R15GM066279, R01GM080295).

References

1. Alexander C, Andersson HS, Andersson LI, Ansell RJ, Kirsch N, Nicholls IA, O'Mahony J, Whitcombe MJ. *J. Mol. Recognit.* 2006; 19:106–180. [PubMed: 16395662]
2. Zhang H. *Eur. Polym. J.* 2013; 49:579–600.
3. Pérez-Moral N, Mayes AG. *Macromol. Rapid Commun.* 2007; 28:2170–2175.
4. Hoshino Y, Kodama T, Okahata Y, Shea KJ. *J. Am. Chem. Soc.* 2008; 130:15242–15243. [PubMed: 18942788]
5. Ma Y, Pan G, Zhang Y, Guo X, Zhang H. *Angew. Chem. Int. Ed.* 2013; 52:1511–1514.
6. Zhao Y, Ma Y, Li H, Wang L. *Anal. Chem.* 2012; 84:386–395. [PubMed: 22092222]
7. Matsui J, Akamatsu K, Nishiguchi S, Miyoshi D, Nawafune H, Tamaki K, Sugimoto N. *Anal. Chem.* 2004; 76:1310–1315. [PubMed: 14987086]
8. Tokonami S, Shiigi H, Nagaoka T. *Anal. Chim. Acta.* 2009; 641:7–13. [PubMed: 19393361]
9. Xu L, Pan J, Xia Q, Shi F, Dai J, Wei X, Yan Y. *J. Phys. Chem. C.* 2012; 116:25309–25318.
10. Zhang W, Li Y, Wang Q, Wang C, Wang P, Mao K. *Environ. Sci. Pollut. Res. Int.* 2013; 20:1431–1440. [PubMed: 22645011]
11. Gonzato C, Courty M, Pasetto P, Haupt K. *Adv. Funct. Mater.* 2011; 21:3947–3953.
12. Liu Y, Huang Y, Liu J, Wang W, Liu G, Zhao R. *J. Chromatogr. A.* 2012; 1246:15–21. [PubMed: 22321951]
13. Lu C-H, Wang Y, Li Y, Yang H-H, Chen X, Wang X-R. *J. Mater. Chem.* 2009; 19:1077–1079.
14. Xu C, Shen X, Ye L. *J. Mater. Chem.* 2012; 22:7427–7433.
15. Xu C, Ye L. *Chem. Commun.* 2011; 47:6096–6098.
16. Maalouli N, Barras A, Siriwardena A, Bouazaoui M, Boukherroub R, Szunerits S. *Analyst.* 2013; 138:805–812. [PubMed: 23223216]
17. Baruah H, Puthenveetil S, Choi YA, Shah S, Ting AY. *Angew. Chem. Int. Ed.* 2008; 47:7018–7021.
18. Madwar C, Kwan WC, Deng L, Ramström O, Schmidt R, Zou S, Cuccia LA. *Langmuir.* 2010; 26:16677–16680. [PubMed: 20964389]
19. Holzinger M, Abraha J, Whelan P, Graupner R, Ley L, Hennrich F, Kappes M, Hirsch A. *J. Am. Chem. Soc.* 2003; 125:8566–8580. [PubMed: 12848565]
20. Joester D, Klein E, Geiger B, Addadi L. *J. Am. Chem. Soc.* 2006; 128:1119–1124. [PubMed: 16433527]

21. Liu L, Engelhard MH, Yan M. *J. Am. Chem. Soc.* 2006; 128:14067–14072. [PubMed: 17061889]
22. Liu LH, Lerner MM, Yan M. *Nano Lett.* 2010; 10:3754–3756. [PubMed: 20690657]
23. Kubo T, Wang X, Tong Q, Yan M. *Langmuir.* 2011; 27:9372–9378. [PubMed: 21699222]
24. Liu L, Yan M. *Acc. Chem. Res.* 2010; 43:1434–1443. [PubMed: 20690606]
25. Pastine SJ, Okawa D, Kessler B, Rolandi M, Llorente M, Zettl A, Fréchet JM. *J. Am. Chem. Soc.* 2008; 130:4238–4239. [PubMed: 18331043]
26. Bielecki RM, Doll P, Spencer ND. *Tribol. Lett.* 2013; 49:273–280.
27. Plachinda P, Evans D, Solanki R. *Solid-State Electron.* 2012; 79:262–267.
28. Suggs K, Reuven D, Wang X-Q. *J. Phys. Chem. C.* 2011; 115:3313–3317.
29. Keana JFW, Cai SX. *J. Org. Chem.* 1990; 55:3640–3647.
30. Yoshimatsu K, Reimhult K, Krozer A, Mosbach K, Sode K, Ye L. *Anal. Chim. Acta.* 2007; 584:112–121. [PubMed: 17386593]
31. Uddin KMA, Ye L. *J. Appl. Polym. Sci.* 2013; 128:1527–1533.

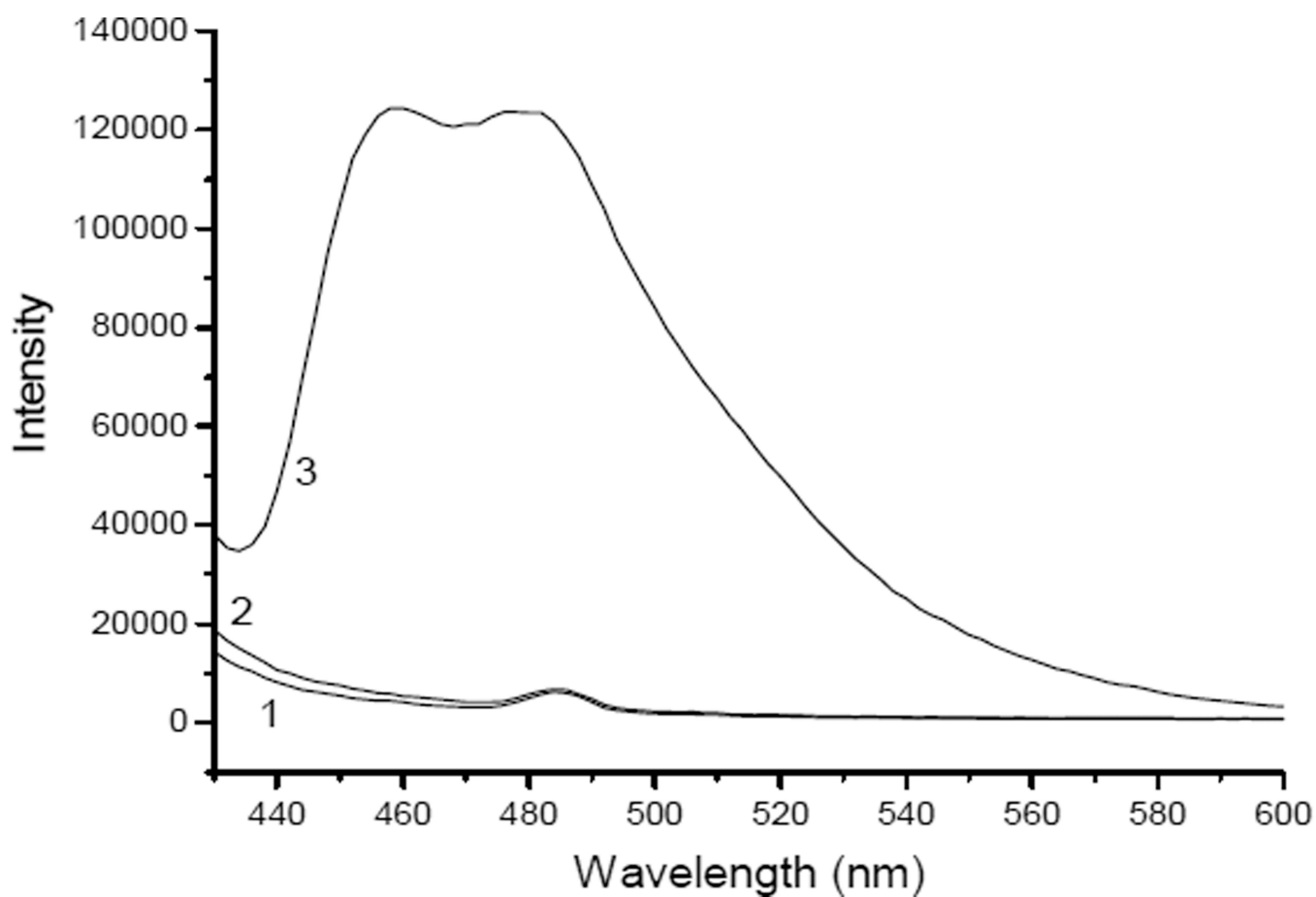


Figure 1. Detection of primary amino groups using the NDA assay. Emission spectra obtained were from sample 1: NDA, sample 2: Fe₃O₄@SiO₂, and sample 3: Fe₃O₄@SiO₂@PAA.

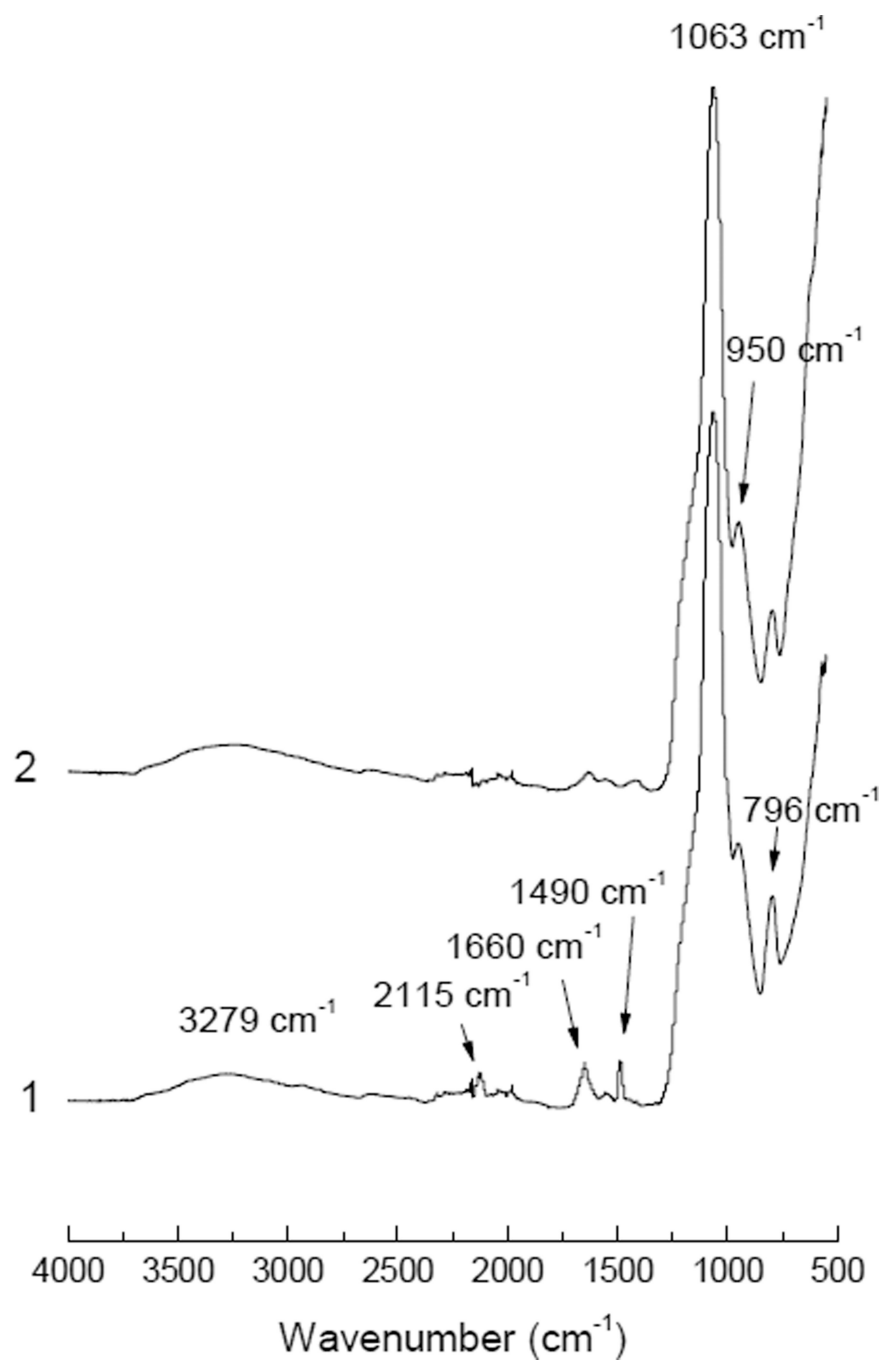


Figure 2. FTIR spectra of $\text{Fe}_3\text{O}_4@SiO_2@PAA@PFPA$ (1) and $\text{Fe}_3\text{O}_4@SiO_2@PAA$ (2).

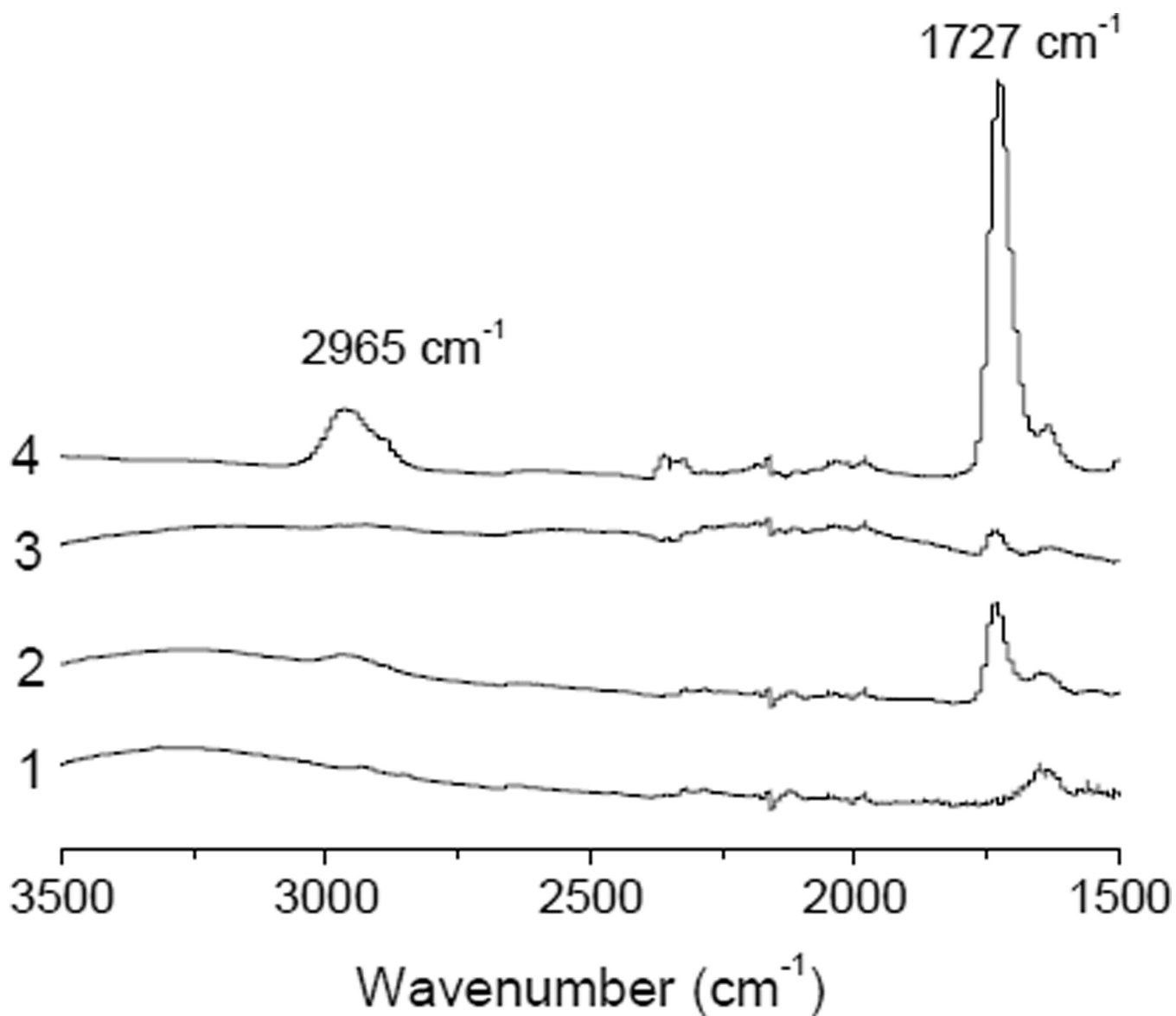


Figure 3. FTIR spectra of: (1) $\text{Fe}_3\text{O}_4@\text{SiO}_2@\text{PAA}@\text{PFPA}$, (2) magnetic MIP composite, (3) mixture of MIP nanoparticles and $\text{Fe}_3\text{O}_4@\text{SiO}_2@\text{PAA}@\text{PFPA}$ after magnetic separation, and (4) MIP nanoparticles.

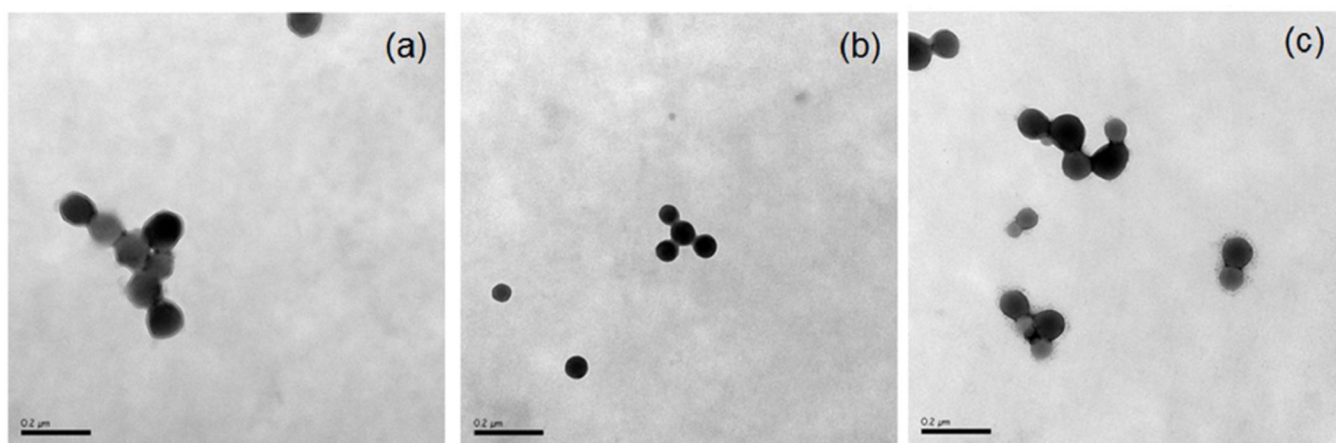


Figure 4. TEM images of MIP (a), $\text{Fe}_3\text{O}_4@SiO_2@PAA@PFPA$ (b) and magnetic MIP composite (c). The scale bar represents 200 nm.

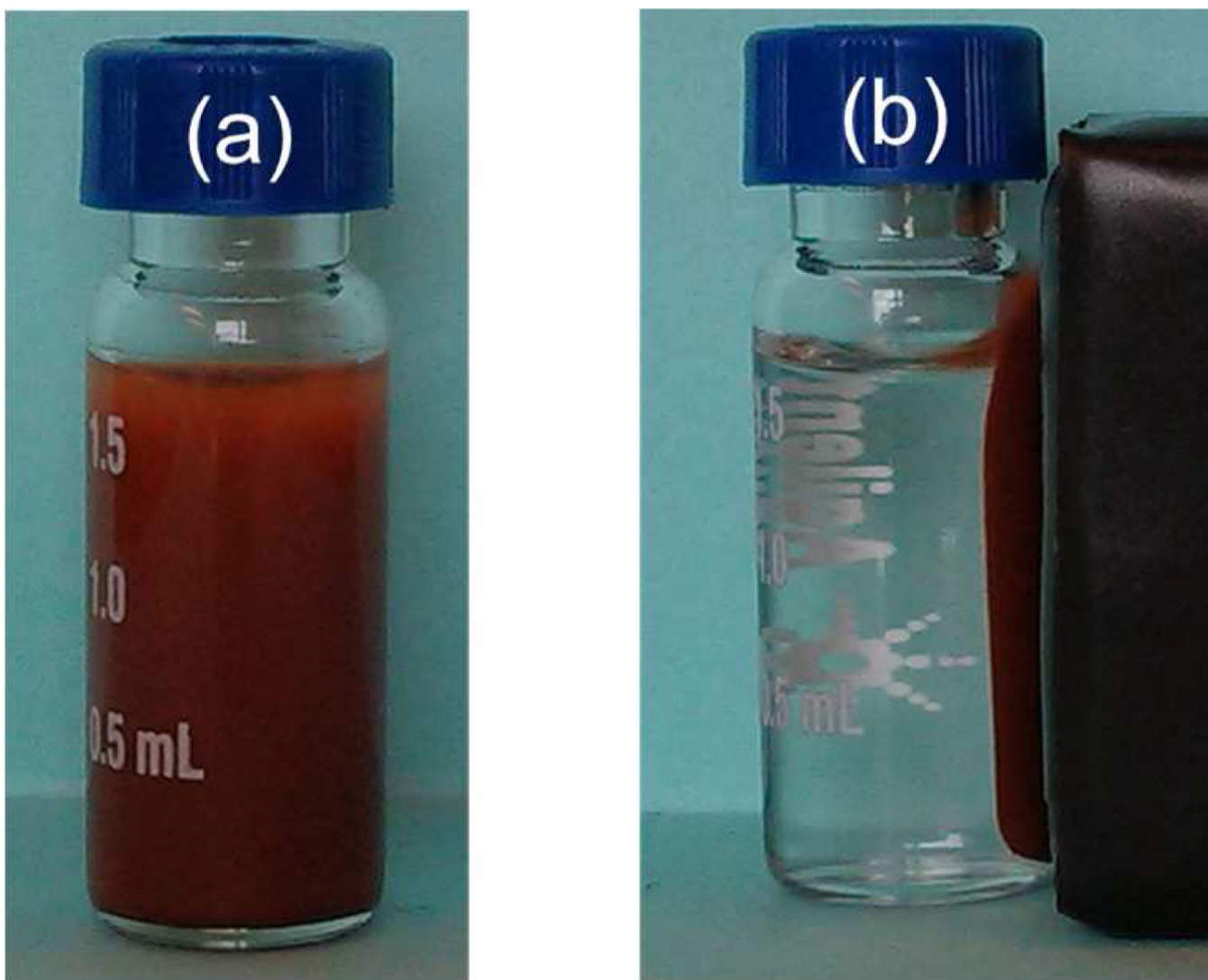


Figure 5. A suspension of photoconjugated particles before (a) and after (b) being exposed to a permanent magnet for 1 min. Image (a) was taken 10 min after the sample was agitated.

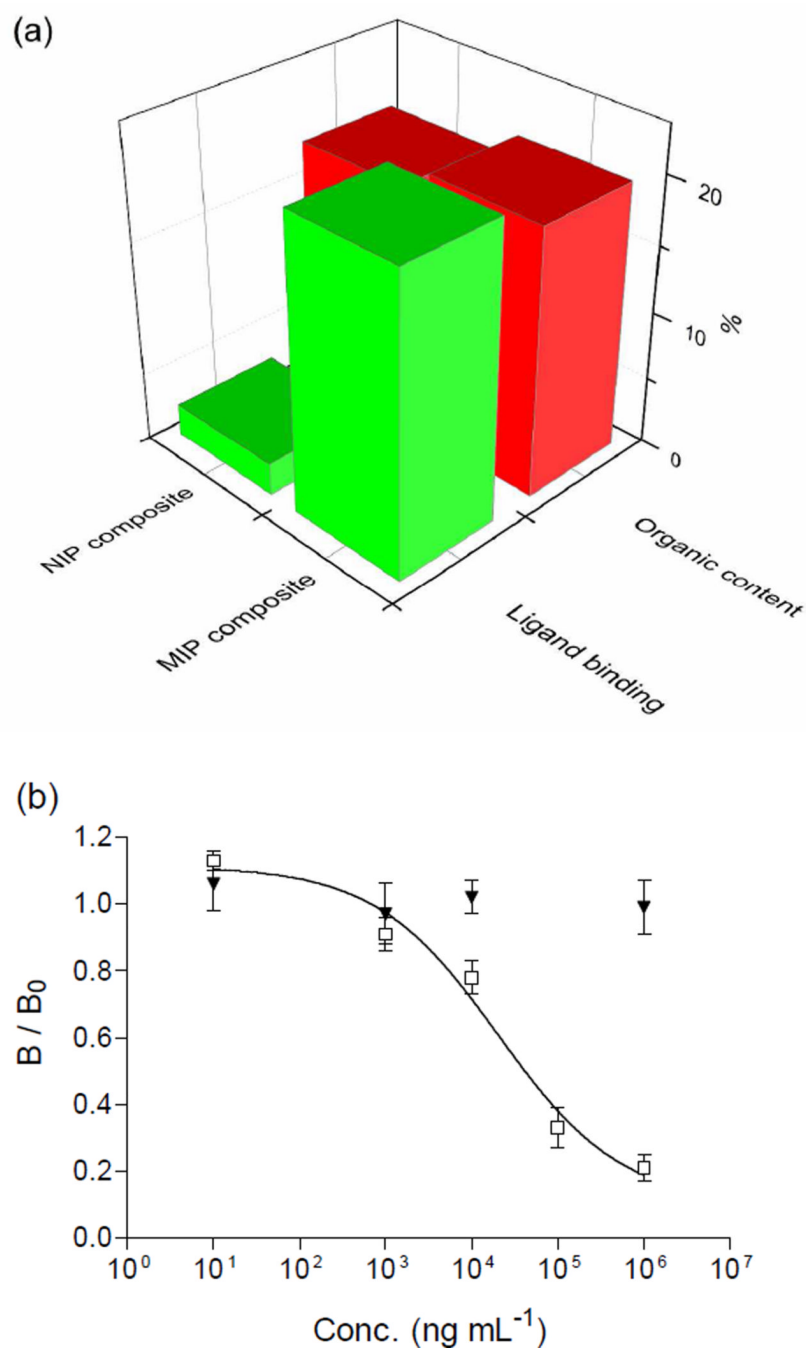
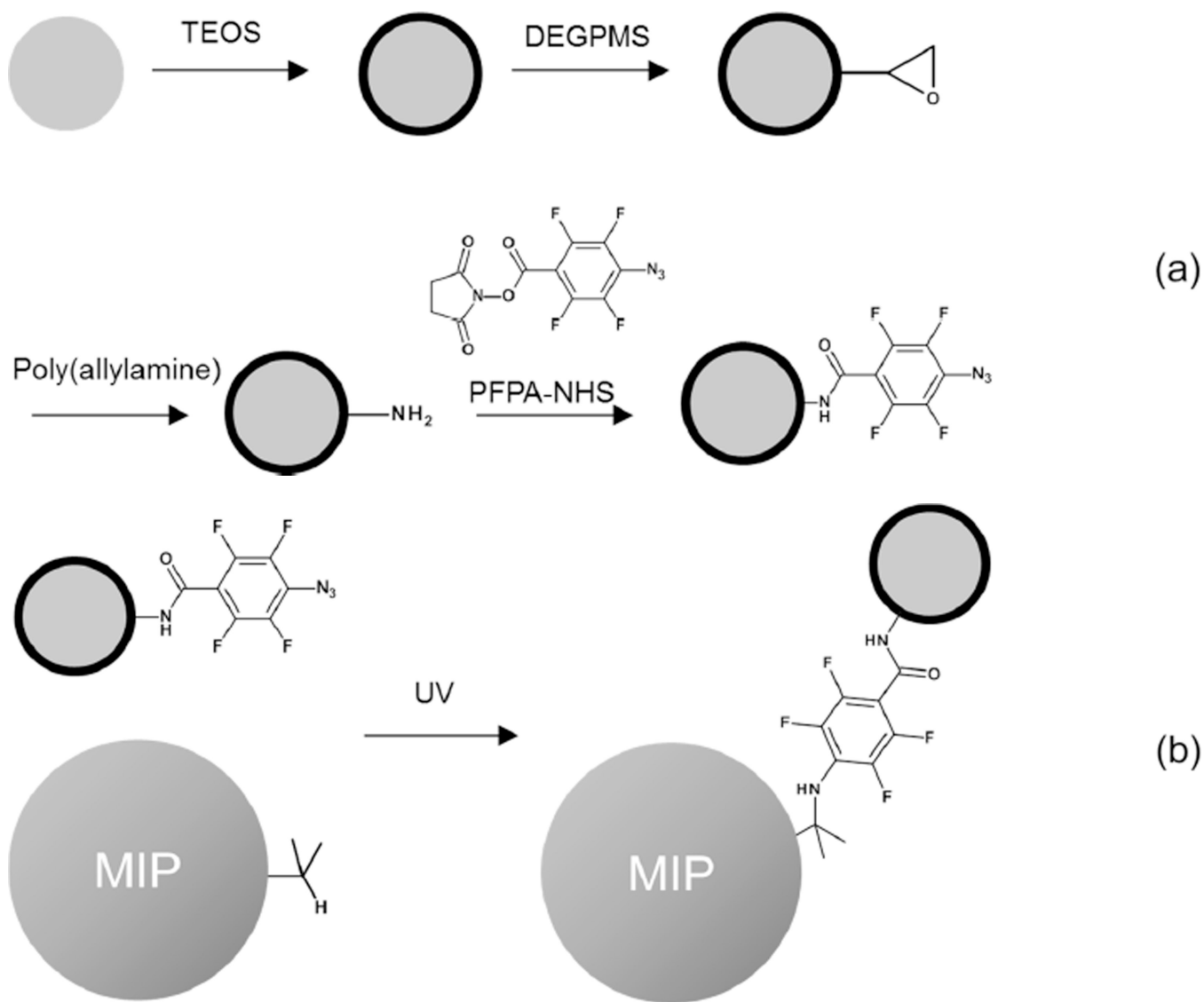


Figure 6. (a) Uptake of radioligand (S)-propranolol by the photoconjugated composite particles. (b) Displacement of (S)-[4-³H]-propranolol from magnetic MIP composite by (S)-propranolol (□) and atenolol (▼). B and B₀ are the amount of bound radioligand in the presence and absence of the competing compounds, respectively. The error bar indicates standard deviation (n = 3).

**Scheme 1.**

(a) Preparation of $\text{Fe}_3\text{O}_4@SiO_2@PAA@PFPA$. (b) Photoconjugation of MIP nanoparticle with PFPA-modified magnetic nanoparticle.